Regular Article

Area-law-like systems with entangled states can preserve ergodicity

Andre M.C. Souza[1,2,a], Peter Rapčan[1,3], and Constantino Tsallis[1,4,5]

[1] Centro Brasileiro de Pesquisas Físicas and National Institute of Science and Technology for Complex Systems, Rua Dr. Xavier Sigaud 150, 22290-180 Rio de Janeiro, Brazil
[2] Departamento de Fisica, Universidade Federal de Sergipe, 49100-000 Sao Cristovao, Brazil
[3] Institute of Physics, Slovak Academy of Sciences, Dúbravská cesta 9, 841 04 Bratislava, Slovak Republic
[4] Santa Fe Institute, 1399 Hyde Park Road, Santa Fe, NM 87501, USA
[5] Complexity Science Hub Vienna, Josefstadter Strasse 39, 1080 Vienna, Austria

Abstract. We study the ground entangled state of the one-dimensional spin-1/2 Ising ferromagnet at its transverse-field critical point. When this problem is expressed in terms of independent fermions, we show that the usual thermostatistical sums emerging within Fermi-Dirac statistics can, for an L-sized subsystem, be indistinctively taken up to L terms or up to $\ln L$ terms, providing a neat understanding of the origin of the logarithmic scaling of the entanglement entropy in the system. This is interpreted as a compact occupancy of the phase-space of the L-subsystem, hence standard Boltzmann-Gibbs thermodynamics quantities with an effective system size $V \propto \ln L$ are appropriate and are explicitly calculated. The calculations are then to be done in a Hilbert space whose effective dimension is $2^{\ln L}$ instead of 2^L. In this we can assume ergodicity. Our analysis suggests a scenario where the physical systems are essentially grouped into three classes, in terms of their phase-space occupancy, ergodicity and Lebesgue measure.

1 Introduction

The Boltzmann-Gibbs (BG) theory refers to ensembles, which constitute pillars of statistical mechanics [1]. The microcanonical ensemble, for example, is associated with the set of points in the phase-space in which one can choose a given total energy. In this case, the ergodic hypothesis is assumed a priori, in which the trajectories of the particles cover the hypersurface of the phase-space corresponding to that energy in a time scale sufficient to carry out measurements. In many cases, it is not necessary for the system to cover the entire phase-space associated with the ensemble in question, but only a finite part of it, for instance half of it. A typical example is usual phase transitions. Below a certain critical temperature, the system has a spontaneous symmetry

[a] e-mail: amcsouza@ufs.br

breaking and effectively occupies only half the phase-space. However, we may still assume the ergodic hypothesis in this half, and thus remain within the BG theory.

A more complex situation occurs in disordered glass-like systems [2], in which the particles cover a small volume of the phase-space corresponding to a vanishing Lebesgue measure [3]. In this case, we can think of two situations: (i) the particles have trajectories that cover a compact subspace of the total phase-space, or, (ii) the particles have trajectories that do not cover the total phase-space, at all relevant time scales, and it is not possible to identify a compact subspace. In studies of conservative nonlinear dynamical systems, some examples of this latter situation have been found [4]. In this case, ergodicity might be broken in such a complex manner that the use of BG theory may be not legitimate. Weak chaotic regimes have been found and the q-statistical generalization [5] of the BG theory has emerged as an appropriate description.

For quantum statistical physics ergodicity has its own nuances in a world where trajectories are not well-defined. For example, the impossibility of energy and particle transport through the total system can lead, among other things, to the breakdown of ergodicity [6–8]. One of the lines of analysis of the ergodicity of quantum physical systems is the study of the entanglement entropy [9–15].

Here, we construct the standard Boltzmann-Gibbs approach associated with the effective tight-binding Hamiltonian, coming from entanglement analysis of the one-dimensional transverse-field spin-1/2 Ising ferromagnet at its zero-temperature critical point [16,17]. We consider an L-sized subsystem of a N-sized ring, and trace over the states of $(N - L)$ spins, with $N \to \infty$. The full N-system is in a pure state, but the L-system is in a statistical mixture due to the entanglement of the ground state. Thus, the subsystem (L-system) can be presented as a finite temperature free fermions system.

The entropy of the subsystem is known to follow the area law with a logarithmic correction, i.e. a behavior qualitatively different from the volume law. We show that the nature of the states is such that a part of the fermionic modes is practically trapped in their ground states while their respective excited states are physically unattainable. These modes thus constitute a frozen, thermodynamically inactive, part of the phase-space. In this sense, particles are localized, however without destroying the nature of the phase-space occupancy, covering a *compact* subspace of the total phase-space. Therefore, the BG theory can continue to be legitimately used. In this case, we can recover extensivity for physical quantities such as the entropy, which can be made to grow linearly with the system size, if one redefines the size of the system so that it does not count the thermodynamically inactive modes.

We emphasize that, in this work, by the expression phase-space we shall mean either a proper classical phase-space, or a quantum mechanical Hilbert space.

The rest of this work is organized as follows: In Section 2 we present the transverse-field Ising model, a brief review of the entanglement analysis and a numerical study at critical point for this model. Section 3 describes the construction of the standard Boltzmann-Gibbs approach associated with the effective tight-binding Hamiltonian, coming from entanglement analysis of the transverse-field Ising model, where we emphasize the adequacy of an effective system size. Finally, Section 4 closes the work with our concluding remarks.

2 The transverse-field Ising model and entanglement analysis

2.1 Literature review

The one-dimensional transverse-field spin-1/2 Ising ferromagnet with N sites is described by the following Hamiltonian [16]

$$\hat{H} = -\sum_{i=0}^{N-1} \left(\sigma_i^x \sigma_{i+1}^x + \lambda \sigma_i^z \right), \tag{1}$$

where σ_i^α is the αth Pauli matrix at site i and λ denotes the magnetic field along the z direction. The Hamiltonian (1) can be diagonalized by a Jordan-Wigner transformation [17].

The ground-state properties of this model strongly depend on λ. A zero-temperature quantum phase transition occurs when $\lambda = 1$ in the $N \to \infty$ limit. The ground-state behavior is further revealed by the interplay between entanglement and the ground-state structure [14]. Right at the critical point, $\lambda = 1$, the spins are mostly entangled and, in this case, it is possible to define a proper entanglement witness which brings about signatures of a quantum phase transition.

One of the most commonly-used entanglement measures for such a task is the von Neumann entropy of a subsystem, also referred to as the entanglement entropy in the literature [9–15]. Given a system in a pure state, it quantifies how much its subsystem, which can be properly described by a reduced density matrix, is entangled with the remaining part of the system. For a spin chain with N sites, we obtain the state describing a given block of L spins ρ_L by tracing out the subsystem of length $(N - L)$ of the overall density matrix ρ_N. We have taken the thermodynamic limit $(N \to \infty)$.

The von Neumann entanglement entropy reads [10]

$$S_{vN}(L, \lambda) = -Tr[\rho_L \ln(\rho_L)]. \tag{2}$$

Note that many other entanglement measures can be defined [20], such as the Rényi entropy [18,19] and the related q-entropy [5] which we discuss later. Regardless of the choice though, all the relevant information is contained in the reduced density matrix ρ_L.

We stress that, when quantifying entanglement via the von Neumann entropy, there is no need to impose extra conditions in order to establish a connection with thermodynamics. Here, we will show the entanglement entropy naturally assumes the role of thermodynamic entropy as well, by allowing for extensive thermodynamic variables corresponding to an effective volume of the system.

Away from the critical point, that is $\lambda \neq 1$ (recall that $L \to \infty$), it is possible to express ρ_L as a tensor product of density matrices accounting for uncorrelated spinless free fermionic modes [13], i.e, $\rho_L = \otimes_n \tilde{\rho}_n$. The energy of a fermion present in the nth mode reads

$$\epsilon_\lambda(n) = \begin{cases} (2n + 1)\epsilon_\lambda, & \text{for } \lambda < 1, \\ 2n\epsilon_\lambda, & \text{for } \lambda > 1, \end{cases} \tag{3}$$

with $n = 0, 1, 2, \ldots$ and

$$\epsilon_\lambda = \pi \frac{I(\sqrt{1 - y^2})}{I(y)}, \tag{4}$$

where

$$I(y) = \int_0^1 \frac{dx}{\sqrt{(1 - x^2)(1 - y^2 x^2)}} \tag{5}$$

is the complete elliptic integral of the first kind and $y = \min[\lambda, \lambda^{-1}]$, where the density matrices read

$$\tilde{\rho}_n = \frac{1}{1 + e^{-\epsilon_\lambda(n)}} \begin{pmatrix} 1 & 0 \\ 0 & e^{-\epsilon_\lambda(n)} \end{pmatrix}. \tag{6}$$

Once we have obtained the reduced density matrix, we can calculate the von Neumann entropy for, say, $\lambda > 1$, using

$$S_{vN}(\infty, \lambda) = \sum_{n=0}^{\infty} \left[\ln\left(1 + e^{-2n\epsilon_\lambda}\right) + \frac{2n\epsilon_\lambda}{1 + e^{2n\epsilon_\lambda}} \right]. \tag{7}$$

In the vicinity of the critical point ($\lambda \to 1$), we have that $\epsilon_\lambda \to 0$ and the sum above can be approximated by the integral

$$S_{vN}(\infty, \lambda) \simeq \int_0^{\infty} dx \left[\ln\left(1 + e^{-2x\epsilon_\lambda}\right) + \frac{2x\epsilon_\lambda}{1 + e^{2x\epsilon_\lambda}} \right] \tag{8}$$

$$S_{vN}(\infty, \lambda) \simeq \frac{\pi^2}{12\epsilon_\lambda} \to \infty. \tag{9}$$

Note that the asymptotic result of equation (9) remains valid if one takes the $\lambda < 1$ variants of equations (7) and (8) and Taylor expands the result of the so obtained integral around $\epsilon_\lambda = 0$. With respect to the $\lambda > 1$ case, the said expansion differs only by extra $O(\epsilon_\lambda^0)$ and higher-order terms, which are discarded in the asymptotic result anyway. Similarly to the von Neumann entropy, one can unveil the behavior of the Rényi and of the q-entropy by a similar procedure [21,22].

At the critical point, a similar analysis can be carried out. By considering now an L-sized subsystem, its reduced density matrix ρ_L is obtained from the following matrix [10,12]

$$\Gamma_L = \begin{pmatrix} \Pi_0 & \Pi_1 & \cdots & \Pi_{L-1} \\ \Pi_{-1} & \Pi_0 & & \vdots \\ \vdots & & \ddots & \vdots \\ \Pi_{1-L} & \cdots & \cdots & \Pi_0 \end{pmatrix}, \tag{10}$$

where

$$\Pi_l = \begin{pmatrix} 0 & \frac{-4}{\pi(2l+1)} \\ \frac{-4}{\pi(2l-1)} & 0 \end{pmatrix}. \tag{11}$$

An orthogonal matrix transforms Γ_L into a block-diagonal matrix with purely imaginary eigenvalues $\pm i\nu_n$ ($n = 1, .., L$).

The 2^L eigenvalues of ρ_L are given by

$$\mu_{x_1 x_2 ... x_L} = \prod_n \frac{1 + (-1)^{x_n} \nu_n}{2} \tag{12}$$

where $x_n = 0, 1 \; \forall n$.
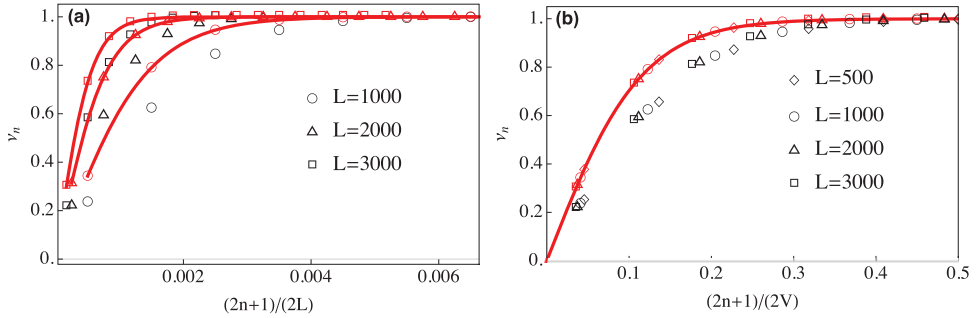
Fig. 1. (a) Positive eigenvalues of Γ_L/i as a function of $(2n+1)/2L$ for $L = 1000$, 2000 and 3000. Lower symbols (black online) represent the results obtained by numerical diagonalization, while the upper ones (red online) denote the theoretical result $\nu_n = \tanh[(2n+1)\epsilon_L/2]$, where ϵ_L is given by equation (17). (b) The same as in panel (a) but the abscissa is $(2n+1)/2V$ with $V = 1.77\ln(L)$. $n = 0, .., L-1$. Curves in both panels represent the theoretical results plotted for real values of the abscissa variable. Due to $\epsilon_L \propto V$ with an L-independent proportionality constant, the argument of the theoretical ν_n is a constant (say α-) multiple of the abscissa variable in panel (b). Hence, in panel (b), all theoretical ν_n lie on a single L-independent curve, $\tanh[\alpha \cdot]$. In the $L \to \infty$ limit, the numerical values will touch the theoretical curve at points coinciding with the respective theoretical values of ν_n.

2.2 Numerical analysis at the critical point

In Figure 1a we show the positive eigenvalues ν_n of Γ_L/i, depicted by the lower symbols (black online), obtained through a straightforward numerical diagonalization for various block sizes. Analogously to the $\lambda \neq 1$ case, at the critical point the model can also be mapped onto a system featuring spinless free fermions and thus $\rho_L = \otimes_n \hat{\rho}_n$, where $\hat{\rho}_n$ has a form analogous to that of equation (6), with $\epsilon_\lambda(n)$ being replaced by a so far undefined symbol $\epsilon_L(n)$. It is well known [23] that the single-mode energies $\epsilon_L(n)$ can be obtained by the inverse of the expression

$$\nu_n = \tanh[\epsilon_L(n)/2] \tag{13}$$

from the numerically acquired values ν_n. Note that the $\{\epsilon_L(n)\}$ are sometimes, and more correctly, referred to as single-particle pseudoenergies in the literature due to being the eigenvalues of the so-called *effective* single-particle Hamiltonians, we refer to them simply as energies for the sake of brevity.

Figure 2 shows the quantity $\epsilon_L(n)$ as a function of L. For all L that we were able to access numerically, we obtained a non-linear single-mode energy spectrum. However, for the low-lying energies – roughly defined as those associated with the modes having non-negligible contribution to the entropy of the subsystem – the non-linearity was vanishing with increasing L. The numerics strongly suggests a linear spectrum in this low-lying part of the spectrum at infinite L. The difference $\epsilon_L(n) - \epsilon_L(n-1)$ as a function of n is shown in Figure 3 for different values of L. We observe that with increasing L this difference tends to a constant value, and for each sufficiently large L we can replace the function $\epsilon_L(n)$ by an expression linear in n for a vanishingly small fraction of all modes – those within $0 \leq n/L \leq V/L$, where $V \propto \ln(L)$ will be obtained later on. Combining this numerical evidence with the above analytical results for the relation between the coefficients of the linear expression, for large L,
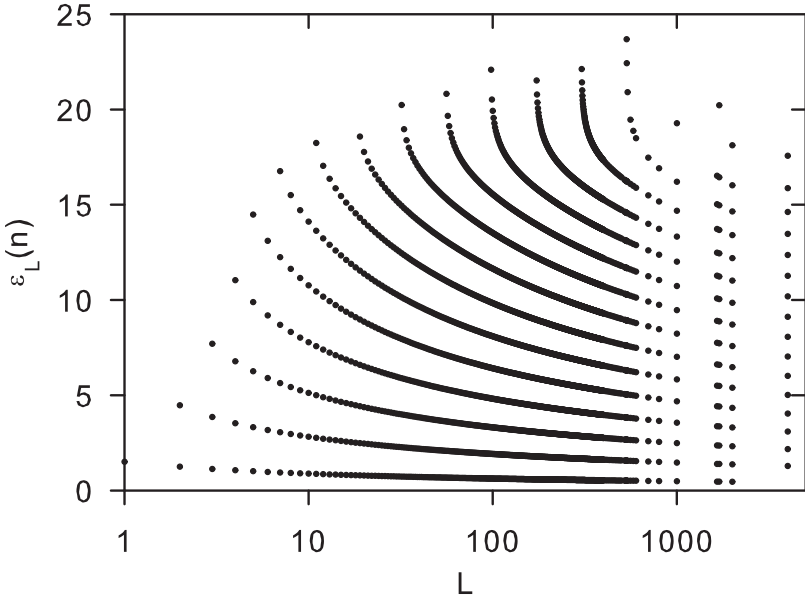
Fig. 2. $\epsilon_L(n)$ as a function of L for different values of n.
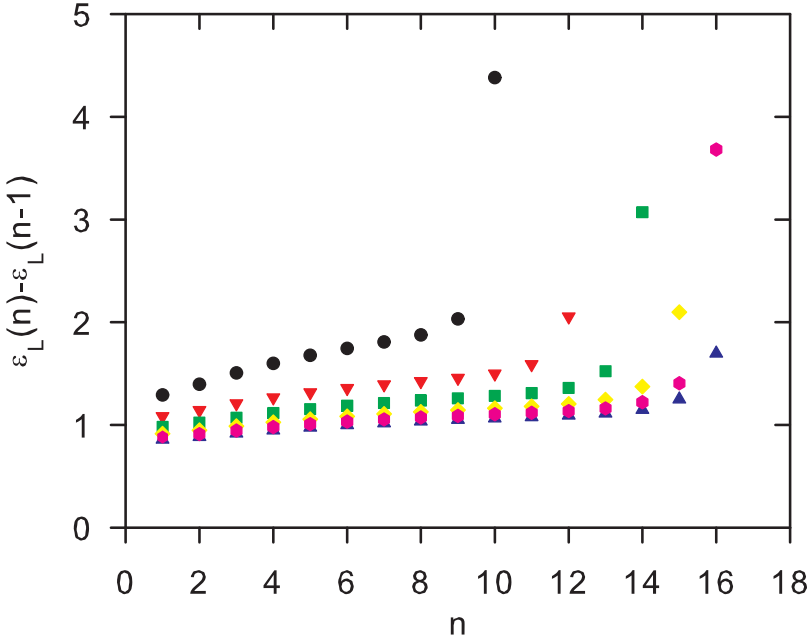
Fig. 3. The difference $\epsilon_L(n) - \epsilon_L(n-1)$ as a function of n for $L = 100$ (black circles), $L = 400$ (red downward-pointing triangles), $L = 1000$ (green squares), $L = 2000$ (yellow diamonds), $L = 3000$ (pink hexagons), and $L = 4000$ (blue upward-pointing triangles).

and for the relevant range of the values of n, we can write the energy spectrum as

$$\epsilon_L(n) \approx (2n+1)\epsilon_L. \tag{14}$$

Such linear spectrum was obtained by Peschel [23] for a matrix commuting with Γ_L, the spectrum of which he showed to be proportional to the spectrum of Γ_L if one restricts oneself to the low lying part of the spectra. We obtained the free parameter $\epsilon_L \equiv \epsilon_L(0)$ theoretically, observing that $\epsilon_L \to 0$ for $L \to \infty$, so that, analogously to equations (7), (8), and (9), we can write

$$S_{vN}(L,1) \simeq \frac{\pi^2}{12\epsilon_L}. \tag{15}$$

Using that [10,13]

$$S_{vN}(L,1) \simeq \frac{1}{6}\ln(L), \tag{16}$$

we obtain

$$\epsilon_L \simeq \frac{\pi^2}{2\ln(L)}. \tag{17}$$

Our analytical results for the eigenvalues of Γ_L/i, based on equation (13) and on the spectrum given by equations (14) and (17), are represented by the upper shapes (red online) in Figure 1a, while the actual eigenvalues, obtained by numerical diagonalization of Γ_L/i, are represented by the shapes (black online) below the analytical ones. Note that the match between the analytical values and the numerical values is far from perfect due to finite-size effects. The entropy in equation (16) is an asymptotic expression neglecting $O(1)$ terms. In other words, our analytical result is only an asymptotic one, and the condition $\ln(L) \gg 1$ is implicitly assumed. That condition is clearly not quite met at $\ln(3000) \approx 8$, hence a deviation from the asymptotic behavior in the plotted finite-size regime is to be expected.

The numerics further shows that, for large enough L, the values of $\epsilon_L(n)$ beyond the low-lying part of the single-particle spectra are in fact lower bounded by the linear relation in equation (14). Moreover, the probability of a fermion being present in the mode n is given by $(1 - \tanh[\epsilon_L(n)/2]/2) \simeq \exp[-\epsilon_L(n)]/2$, and thus vanishes approximately exponentially in n already for high enough modes of linear spectra, and even faster for the corresponding modes of the exact spectra. Therefore, only a vanishing error will be introduced in terms of the entropy of the subsystem, or in terms of the expectation value of energy, if the spectra are truncated beyond their low lying parts. Let us stress that the region of higher energies is thus thermodynamically irrelevant, and can be dropped from the description altogether for large enough L-systems, as we shall confirm below.

3 The standard Boltzmann-Gibbs approach associated with the effective model

We can think of the problem not solely for the purpose of entanglement analysis, but also regarding the spin block as a physical system of interest by itself. In general, for an arbitrary system, the entanglement entropy of the subsystem does not equal its thermodynamic entropy. However, in the present study, we show that this equality is valid. Thus, it becomes relevant to discuss its thermodynamic properties, which is carried out in what follows. We have a system of L free fermions whose Hamiltonian reads as

$$\hat{H}_L = E_L \sum_{n=0}^{L-1} (2n+1)\hat{c}_n^\dagger \hat{c}_n, \tag{18}$$

where $\hat{c}_n^\dagger$ ($\hat{c}_n$) are the creation (annihilation) fermionic operators at site n for a one-dimensional lattice. $E_L = \epsilon_L \epsilon_0$, where both ϵ_0 and $\hat{H}_L$ have the dimension of energy.

The Hamiltonian (18) represents tightly-bounded electrons in a uniform electric field [24,25]. This model has been extensively studied, both on theoretical and experimental grounds (see, e.g., [26,27]). Our case, however, embodies the limit of localized atomic electrons, where nearest-neighbor hopping is neglected. In this extreme limit, the equidistant energy levels are identified as Stark ladders [28]. The concept of Stark ladder was put forward by Wannier [29] and confirmed experimentally in several setups, for instance, in GaAs-GaAlAs superlattices subjected to electric fields [26] and in an elastic-rod apparatus [27].

The thermodynamic properties of the free fermions at temperature T are determined from the partition function of the canonical ensemble

$$Z(L) = Tr[e^{-\beta \hat{H}_L}] = \prod_{n=0}^{L-1} \left(1 + e^{-\beta(2n+1)E_L} \right), \qquad (19)$$

where $\beta = 1/(k_B T)$. We obtain the Helmholtz free energy

$$F(L) = -\frac{1}{\beta} \ln[Z(L)] = -\frac{1}{\beta} \sum_{n=0}^{L-1} \ln \left[1 + e^{-\beta(2n+1)E_L} \right] \qquad (20)$$

and the internal energy

$$U(L) = -\frac{\partial}{\partial \beta} \ln[Z(L)] = \sum_{n=0}^{L-1} \frac{(2n+1)E_L}{1 + e^{\beta(2n+1)E_L}}. \qquad (21)$$

As in equation (8), the above sums can be approximated by integrals and we obtain

$$F(L) \simeq -\frac{\pi^2}{24E_L\beta^2} = -\frac{1}{12\beta^2\epsilon_0} \ln(L) \qquad (22)$$

and

$$U(L) \simeq \frac{\pi^2}{24E_L\beta^2} = \frac{1}{12\beta^2\epsilon_0} \ln(L). \qquad (23)$$

Consequently, it becomes straightforward to obtain the entropy, which reads

$$S(L) = \frac{1}{T}[U(L) - F(L)] \simeq \frac{k_B}{6\beta\epsilon_0} \ln(L). \qquad (24)$$

One can recover the entanglement entropy by assuming $\beta\epsilon_0 = 1$ and thus $S_{vN}(L,1) \simeq \frac{k_B}{6} \ln(L)$. We can also write the Rényi [18] and q-statistics entropies [21] as

$$S_\alpha^R(L,1) = \frac{1}{1-\alpha} \ln[Tr(\rho_L)^\alpha] \simeq \frac{(\alpha+1)}{12\alpha} \ln(L) \qquad (25)$$
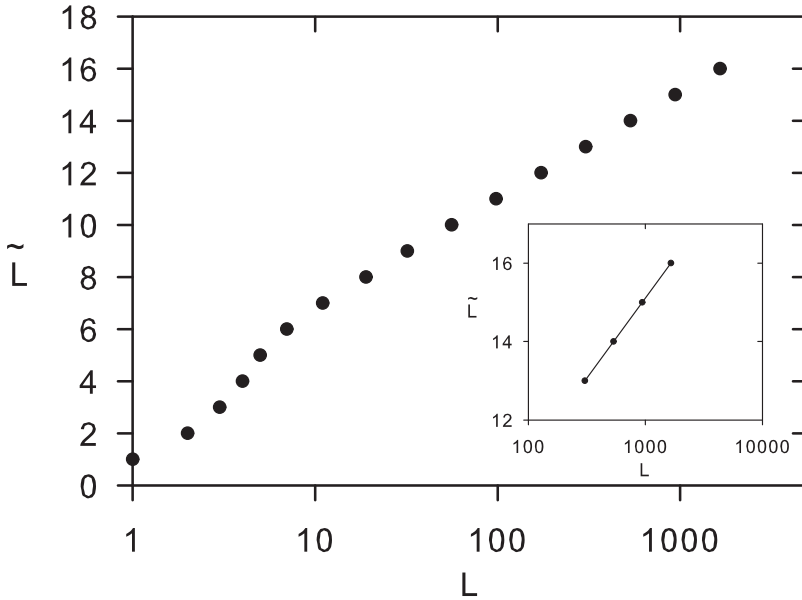
Fig. 4. Number of thermodynamically relevant modes $\tilde{L}$ versus the block size L. Inset: fitting $\tilde{L} = 1.77 \ln L + 2.88$ $(r^2 = 0.999999)$ for $L > 300$.

and

$$S_q(L,1) = \frac{1 - Tr(\rho_L)^q}{q-1} \simeq \frac{L^{(\frac{1}{q}-q)\frac{1}{12}} - 1}{1-q},\tag{26}$$

respectively.

Note that the q-entropy can be used by satisfying the requirement of extensivity, i.e., $(\frac{1}{q} - q)\frac{1}{12} = 1$, hence $q_c = \sqrt{37} - 6 \simeq 0.08$ [21]. In this case,

$$S_{q_c}(L,1) \simeq L,\tag{27}$$

and the desired thermodynamic extensivity is recovered.

As known in the literature, this system has an effective number of unattainable physical energy states, corresponding to the vanishing eigenvalues of the density matrices [12]. Another way to put this is by thinking that we have a set of free-fermionic modes frozen in the ground state that depends on the manner through which entanglement was established in the original problem. Therefore, since only a part of the free fermions becomes thermodynamically accessible, only a subset of the modes effectively contributes to the entropy of the subsystem.

This holds both for the effective model discussed above, as well as for the exact critical Ising model. Figure 4 shows the number of thermodynamically relevant modes $\tilde{L}$ versus the block size L for the exact critical Ising model. For $L > 300$, we obtain numerically (see inset of Fig. 4)

$$\tilde{L} = 1.77 \ln L + 2.88 \quad (r^2 = 0.999999).\tag{28}$$

The points in Figure 4 have been obtained as follows: at infinite (practically at a high enough) precision the positive eigenvalues of Γ_L/i obtained numerically

fulfil the strict inequality $0 < \nu(n) < 1$ for arbitrary finite L. For any fixed computer precision there will exist an integer L' such that, for each $L > L'$, some of the positive eigenvalues will be numerically indistinguishable from 1. Assuming $\nu(n)$ ordered in an ascending order for each L as before, then $\tilde{L}$ in Figure 4 denotes the largest n such that $\nu(n) \neq 1$ if performing the spectrum computation at the given precision, which we have chosen to be the single precision (binary32 floating-point format).

In other words, since the probability of the nth single-particle mode to be occupied is given by $(1 - \nu(n))/2$, at the chosen precision the $\tilde{L}$th mode is the last one contributing to the entropy, or to expectation value of energy (note that each mode's ground state (pseudo)energy is chosen to be 0). Moreover, also the *collective* contribution of the remaining $L - \tilde{L}$ modes – obtained by calculating contributions of the individual modes "exactly" and applying the numerical rounding only to the sum of those individual contributions – would still be negligible (see the discussion at the end of Sect. 2.2). Hence $\tilde{L}$ represents the effective size of the system at the chosen precision, as far as thermodynamical description is concerned.

Similarly, one can obtain the effective system size for the effective model, i.e. assuming linear single-particle spectra. Only in this case, it is also possible to obtain an analytical result. As in the exact critical Ising case, we search for the last mode, denoted $\tilde{n}' = \tilde{L}' - 1$, with a non vanishing occupation probability (we use primed variables, $(.)'$, to distinguish the effective model quantities from those of the exact critical Ising case). Assuming that the single-mode occupation probabilities are expressed with a d-digit precision, the largest excitation probability that will be interpreted by the computer as vanishing is $10^{-d}/2 := \Delta$. Thus we are searching for the n fulfilling the equation

$$\frac{1}{2}(1 - \nu_n) = \Delta, \tag{29}$$

where the LHS is the nth mode's occupation probability, the RHS is the maximal rounding error for that quantity, defined earlier, and with ν_n defined in equation (13). Formally, then,

$$\tilde{L} - 1 \equiv \tilde{n} = \varepsilon_L^{-1}(2\text{arctanh}[1 - 2\Delta]), \tag{30}$$

where $\varepsilon_L^{-1}(.)$ is the inverse function of $\varepsilon_L(n)$ from equation (13). For the exact critical Ising model the two latter functions are unknown analytically. However, for the effective model (asymptotically for the relevant energies of the exact model), by inverting the linear-spectrum expression in equations (14) and (17), one obtains $\varepsilon_L^{-1}(x) = \ln(L)x/\pi^2 - 1/2$. Thus, from equation (30) we have for the effective model

$$\tilde{L}' = \tilde{n}' + 1 = \frac{2\text{arctanh}[1 - 2\Delta]}{\pi^2} \ln L + \frac{1}{2}. \tag{31}$$

To make contact with the numerically obtained effective size $\tilde{L}$ of the exact critical Ising block result of equation (28), one has to use, in equation (30), the maximal rounding error Δ corresponding to the precision with which the mode excitation probabilities were numerically obtained. This is not trivial – the chosen single numerical precision is guaranteed to provide 6 significant decimal digits of precision for the *decimal input* data (defined as the guaranteed precision kept in a conversion decimal→binary→decimal), however without a detailed analysis it is not clear how the rounding errors propagate in the spectra computations.

Nevertheless, the actual rounding error of the excitation probabilities obtained in the single-precision numerical calculations can be estimated by performing all the calculations one more time with a higher precision (say double precision) and inferring the single-precision result rounding error from comparing the two – the correct single-precision Δ being such that if one interpreted the higher-precision ground-states probabilities smaller then Δ as vanishing, one would exactly recover the $\tilde{L}(L)$ dependence in equation (28) that was obtained numerically in the original, single-precision, calculation.

Using the procedure just described we obtain $\Delta \approx 5.32 \times 10^{-8}$. Plugging that into equation (31) we obtain the effective system size of the effective model at single precision to be

$$\tilde{L}' \approx 1.697 \ln(L) + O(1), \tag{32}$$

which is the result valid asymptotically for the exact critical Ising model as well. The result is not far from the scaling in equation (28) obtained numerically for the exact critical Ising case with access to finite $L \leq 3000$, the origin of the discrepancy being the finite-size effects manifested already in Figure 1.

Clearly, the slopes in equations (32) and (28) will depend on the precision chosen. The slope in equation (28) will also depend on the said final-size effects that will disappear gradually with L approaching the regime where $\ln(L) \gg 1$. For large enough L at any finite numerical precision used for the computer calculations, we expect the numerical result to approach the analytical one, equation (32) and, $\tilde{L} \propto \ln L$ to always hold asymptotically. The choice of the numerical precision thus has no influence on the qualitative features we point out next.

Figure 1b shows ν_n (also featured in Fig. 1a) now as a function of $(2n + 1)/(2V)$, where $V \equiv 1.77 \ln L$. We can observe a collapse such that the ν_n of the effective model now lie on a single curve independent of L, which is a consequence of the fact that the abscissa variable $(2n + 1)/(2V)$ is a multiple of the argument of the function in equation (13) for the linear single-particle spectra of the effective model. For the exact critical Ising model the relevant part of the spectra is described by equation (14) exactly only in the thermodynamical limit, therefore for finite L we observe finite-size deviations from the collapse curve that are diminishing with as the system size increases, as expected. Both for the effective model and asymptotically for the exact model, the entire physical behavior of the subsystem composed by L fermionic modes can be completely evaluated by considering only the first V modes, where, for the effective model,

$$\sum_{n=0}^{L-1} \ln \left[1 + e^{-\beta(2n+1)E_L}\right] \cong \sum_{n=0}^{V-1} \ln \left[1 + e^{-\beta(2n+1)E_V}\right] \tag{33}$$

and

$$\sum_{n=0}^{L-1} \frac{(2n+1)E_L}{1 + e^{\beta(2n+1)E_L}} \cong \sum_{n=0}^{V-1} \frac{(2n+1)E_V}{1 + e^{\beta(2n+1)E_V}}. \tag{34}$$

This allows us to write

$$\hat{H}_V = E_V \sum_{n=0}^{V-1} (2n+1)\hat{c}_n^\dagger \hat{c}_n. \tag{35}$$

Using this expression, we confirm that the results of equations (22), (23), (24), (25), and (26) are precisely the same.

The thermodynamic properties are extracted from the free energy

$$F(T,V) = -\frac{k_{\mathrm{B}}^2 T^2}{12\epsilon_0}V, \tag{36}$$

such that

$$S_{BG}(T,V) = -\left(\frac{\partial F}{\partial T}\right)_V = \frac{k_{\mathrm{B}}^2 T}{6\epsilon_0}V \tag{37}$$

and

$$U(T,V) = F + TS = \frac{k_{\mathrm{B}}^2 T^2}{12\epsilon_0}V \tag{38}$$

are extensive thermodynamic quantities. For completeness, we can also define the intensive quantity

$$P(T,V) = -\left(\frac{\partial F}{\partial V}\right)_T = \frac{k_{\mathrm{B}}^2 T^2}{12\epsilon_0}, \tag{39}$$

so that we can write $U = PV$. All the above expressions are consistent with standard thermodynamics.

An interesting question, which is beyond the scope of the present work, is to analyze the transverse field Ising chain away from criticality. In this case, the system has a strict area-law scaling that does not have a logarithmic correction. We expect a change of the effective system size V.

4 Conclusions

The entanglement behavior of the system mandates that only a given part of energy states is thermodynamically relevant. As a consequence, the standard BG quantities are associated with an effective system size $V \propto \ln L$, and the phase-space has an effective dimension $2^{\ln L}$ instead of 2^L. The effective number of microstates grows with L as a power-law, in contrast to the exponential growth corresponding to standard nonentangled systems. This provides an understanding of the origin of the logarithmic scaling of the entanglement entropy in the ground state of the studied system which we expect to remain valid for other critical systems. The whole scenario is strongly reminiscent of an usual phase transition of a spin-$1/2$ d-dimensional system, where the phase-space dimension is 2^{L^d} in the disordered phase, and effectively $2^{L^d/2}$ in the ordered one.

The above analysis suggests a scenario where the physical systems are essentially grouped into three classes, in terms of their phase-space occupancy, ergodicity and Lebesgue measure, namely (i) ergodicity occurs in the entire phase-space or in a *compact* subspace whose Lebesgue measure remains different from zero in the thermodynamic limit; (ii) ergodicity occurs only in a *compact* subspace whose Lebesgue measure vanishes in the thermodynamic limit; and (iii) ergodicity does not occur, the trajectories covering a *noncompact* subspace whose Lebesgue measure vanishes in the thermodynamic limit (typically an hierarchical structure like a multifractal). Figure 5 illustrates these classes with examples for three different sizes of system
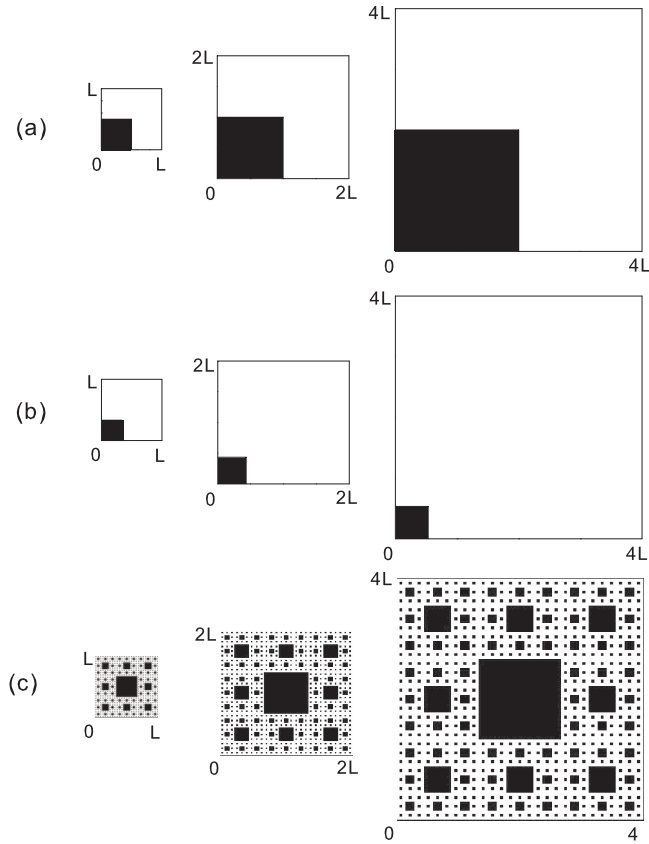
Fig. 5. Classes of the phase-space trajectories covering a (a) *compact* subspace whose corresponding Lebesgue measure remains different from zero in the thermodynamic limit; (b) *compact* subspace whose corresponding Lebesgue measure vanishes in the thermodynamic limit, and; (c) *noncompact* subspace whose corresponding Lebesgue measure vanishes in the thermodynamic limit. Three different size systems are presented.

volume L. Particles of the system cover the hypersurface of the phase subspace corresponding to black color in the figure. For each class, there is an appropriate statistical mechanics. Typical examples of the first class are physical systems with or without usual phase transitions. The BG theory perfectly describes this class and the von Neumann/Boltzmann entropy is an extensive thermodynamic quantity. For systems that fall in the second class, we exhibit in the present work how the BG theory can still be used. Here, we can find a particular value of q such that the q-entropy satisfies the requirement of extensivity within the *total* volume, while the von Neumann/Boltzmann entropy is an extensive thermodynamic quantity within an appropriate *effective* volume. Some of the systems exhibiting the area-law [30,31] for the entropy might also belong to this class. For the third class, we do not expect the use of the BG theory to be legitimate. This is the case for say systems with long-range interactions, for which theories such as q-statistics have been satisfactorily applied [32–34].

Here, the ergodicity in a system whose entanglement entropy obeys the area-law with a logarithmic correction was found by direct analysis at equilibrium. A natural question that arises is to explore directly the dynamics on isolated quantum systems

in the localized phase to show that ergodicity and thermalization may still exist in a small part of a system exhibiting sub volume-law for entanglement.

References

1. L.E. Reichl, *A Modern Course in Statistical Physics*, 3rd edn. (John Wiley & Sons, New York, 2009)
2. R.G. Palmer, Adv. Phys. **31**, 669 (1982)
3. H. Kestelman, *Modern Theories of Integration*, 2nd edn. (Dover, New York, 1960)
4. U. Tirnakli, E.P. Borges, Sci. Rep. **6**, 23644 (2016)
5. C. Tsallis, J. Stat. Phys. **52**, 479 (1988)
6. M. Pouranvari, K. Yang, Phys. Rev. B **89**, 115104 (2014)
7. Z.-C. Yang, C. Chamon, A. Hamma, E.R. Mucciolo, Phys. Rev. Lett. **115**, 267206 (2015)
8. C.R. Laumann, A. Pal, A. Scardicchio, Phys. Rev. Lett. **113**, 200405 (2014)
9. C. Holzhey, F. Larsen, F. Wilczek, Nucl. Phys. B **424**, 443 (1994)
10. G. Vidal, J.I. Latorre, E. Rico, A. Kitaev, Phys. Rev. Lett. **90**, 227902 (2003)
11. A.R. Its, B.-Q. Jin, V.E. Korepin, J. Phys. A **38**, 2975 (2005)
12. J.I. Latorre, E. Rico, G. Vidal, Quantum Inf. Comput. **4**, 48 (2004)
13. P. Calabrese, J. Cardy, J. Stat. Mech. Theory Exp. **2004**, P06002 (2004)
14. L. Amico, R. Fazio, A. Osterloh, V. Vedral, Rev. Mod. Phys. **80**, 517 (2008)
15. R. Islam, R. Ma, P.M. Preiss, M.E. Tai, A. Lukin, M. Rispoli, M. Greiner, Nature **528**, 77 (2015)
16. P. Pfeuty, Ann. Phys. **57**, 79 (1970)
17. S. Sachdev, *Quantum Phase Transitions* (Cambridge Universuty Press, Cambridge, 1999)
18. F. Franchini, A.R. Its, V.E. Korepin, J. Phys. A **41**, 025302 (2008)
19. M.B. Hastings, I. Gonzales, A.B. Kallin, R.G. Melko, Phys. Rev. Lett. **104**, 157201 (2010)
20. R. Horodecki, P. Horodecki, M. Horodecki, K. Horodecki, Rev. Mod. Phys. **81**, 865 (2009)
21. F. Caruso, C. Tsallis, Phys. Rev. E **78**, 021102 (2008)
22. B.-Q. Jin, V.E. Korepin, J. Stat. Phys. **116**, 79 (2004)
23. I. Peschel, J. Stat. Mech. Theory Exp. **2004**, P06004 (2004)
24. H. Fukuyama, R.A. Bari, H.C. Fogedby, Phys. Rev. B **8**, 5579 (1973)
25. M. Saitoh, J. Phys. C Solid State Phys. **6**, 3255 (1973)
26. E.E. Mendez, F. Agullo-Rueda, J.M. Hong, Phys. Rev. Lett. **60**, 2426 (1988)
27. L. Gutierrez, A. Diaz-de-Anda, J. Flores, R.A. Mendez-Sanchez, G. Monsivais, A. Morales, Phys. Rev. Lett. **97**, 114301 (2006)
28. E.O. Kane, J. Phys. Chem. Solids **12**, 181 (1959)
29. G.H. Wannier, Phys. Rev. **117**, 432 (1960)
30. C.M. Herdman, P.-N. Roy, R.G. Melko, A. Del Maestro, Nat. Phys. **13**, 556 (2017)
31. P. Calabrese, M. Mintchev, E. Vicari, Europhys. Lett. **97**, 20009 (2012)
32. C. Tsallis, Eur. Phys. J. Special Topics **226**, 1433 (2017)
33. C. Tsallis, Braz. J. Phys. **39**, 337 (2009)
34. C. Tsallis, *Introduction to Nonextensive Statistical Mechanics* (Springer, Berlin, 2009)